Available online at www.sciencedirect.com
SCIENCE DIRECT
Journal of Molecular Catalysis A: Chemical 248 (2006) 210–219
JOURNAL OF MOLECULAR CATALYSIS A: CHEMICAL
www.elsevier.com/locate/molcata

Structure–activity relationship in the N_2O decomposition over Ni-(Mg)-Al and Ni-(Mg)-Mn mixed oxides prepared from hydrotalcite-like precursors

L. Obalová [a,*], K. Jirátová [b], F. Kovanda [c], M. Valášková [a], J. Balabánová [b], K. Pacultová [a]

[a] *Technical University of Ostrava, 17. listopadu 15, 708 33 Ostrava, Czech Republic*
[b] *Institute of Chemical Process Fundamentals CAS, Rozvojová 135, 165 02 Prague, Czech Republic*
[c] *Department of Solid State Chemistry, Institute of Chemical Technology, Technická 5, 166 28 Prague, Czech Republic*

Received 31 July 2005; received in revised form 21 December 2005; accepted 22 December 2005
Available online 7 February 2006

Abstract

The decomposition of the nitrous oxide over catalysts prepared by thermal decomposition of Ni-(Mg)-M^{III} (M^{III} = Al or Mn) hydrotalcite-like precursors was studied. The mixed oxides obtained at 500 °C were characterized using various techniques—X-ray diffraction (XRD), BET surface area measurements, temperature-programmed desorption (TPD) and temperature-programmed reduction (TPR). The N_2O decomposition was performed in the temperature range 300–450 °C, at 0.05–0.15 mol% inlet N_2O concentrations; oxygen and nitrogen dioxide were added in some runs. The Ni-Al and Mg-Mn catalysts exhibited high catalytic activity but those containing both transition metal cations (i.e. Ni and Mn) were less active. Their lower activity was interpreted in terms of different oxidation states of manganese and nickel in the mixed oxide systems. Up to a certain value of oxygen pressure the presence of oxygen in the reaction mixture caused an inhibition of the reaction rate, while at higher oxygen pressures the N_2O conversion remained nearly constant. The correlation between the observed oxygen inhibition and the proposed N_2O decomposition mechanism as well as the relationship between the observed activity and the amount of reducible components determined from TPR experiments are discussed.

Keywords: N_2O decomposition; Inhibition; Mixed oxide catalysts; Hydrotalcite-like compounds; Layered double hydroxides

1. Introduction

The N_2O decomposition was widely studied in the last three decades because this simple reaction was often chosen as a test reaction for finding a correlation between structural and catalytic properties [1–9]. Recently, the interest in this reaction enhanced since the catalytic decomposition offers an attractive end-of-pipe solution for the abatement of N_2O in waste gases coming from combustion and chemical industry. The state of art in catalytic decomposition of N_2O is well documented in the literature [10,11].

The mechanism of N_2O decomposition is of redox nature as results from published kinetic studies [12,13].

$$N_2O + * \xrightarrow{k_1} N_2 + O^* \quad \text{(R1)}$$

$$O_2 + 2^* \xrightarrow{k_2'} 2O^* \quad \text{(R2)}$$

$$2O^* \xrightarrow{k_2'} O_2 + 2^* \quad \text{(R2′)}$$

$$O^* + N_2O \xrightarrow{k_3} N_2 + O_2 + * \quad \text{(R3)}$$

The catalysts surface can be oxidized either by a molecule of N_2O according to Eq. (R1) (prevailing at very low oxygen pressure) or by an adsorption of the molecular oxygen from gaseous phase according to (R2) (predominating at higher oxygen pressure) [14]. The reduction of the catalyst surface is proposed to follow the Eley–Rideal mechanism (R3) or, alternatively, two adsorbed oxygen atoms can recombine according to Langmuir–Hinshelwood mechanism (R2′). The kinetic models considered by several authors are based on Langmuir–Hinshelwood mechanism [13,15,16], assuming that the surface concentration of the adsorbed oxygen is given by the adsorption equilibria (R2) and (R2′). If the oxygen desorption is the critical step of the process, the presence of labile oxygen on

* Corresponding author. Tel.: +420 59 699 1532; fax: +420 59 732 3396.
E-mail address: lucie.obalova@vsb.cz (L. Obalová).

1381-1169/$ – see front matter © 2006 Elsevier B.V. All rights reserved.
doi:10.1016/j.molcata.2005.12.037

the catalyst surface is necessary to complete the catalytic cycle. On the contrary, Riekert et al. [17] and Golodets [14] speculated that the adsorption equilibrium is not reached because of a too slow desorption of the chemisorbed oxygen (R2′) and therefore, this step (R2′) is of no importance for the overall reaction rate. These authors involved an irreversible adsorption of oxygen (R2) into the reaction scheme instead of the adsorption equilibrium. Uetsuka et al. [18] suggested a recombinative desorption of the surface oxygen via a reaction-assisted desorption. Both the chemisorption of N_2O (R1) and step (R3) were supposed to participate in the overall reaction rate and $k_1 \geq k_3$ was considered [19]. This scenario is in accordance with the transient kinetic experiments carried out by Miller and Grassian [20] and Pérez-Ramírez et al. [21]. It is also important from the point of view of practical use of a catalyst that there is no inhibition of the reaction rate by oxygen present in the reaction mixture. The oxygen inhibition occurs when the rate of oxygen removal from the catalyst surface according to (R3) is slower than step (R1), therefore $k_1 > k_3$. As far as both (R1) and (R3) steps proceed by comparable rates ($k_1 \cong k_3$), the oxygen inhibition does not occur. Accordingly, the bond strength of the surface oxygen turns out to be a crucial factor [10] and hence, the metal oxide catalytic activity for the N_2O decomposition was correlated with the bond energy of the surface oxygen [14] revealing the highest activity of the oxides with lower bond energy. Contrary to it, Vijh [22] showed that the data of the N_2O catalytic decomposition exhibited a volcano-shaped dependence on the heat of formation per oxide equivalent and this correlation were interpreted in terms of the Sabatier–Balandin approach [23,24]. Although the correlation of the catalytic activity with the adsorption heats of the reactants has been frequently applied in catalysis, this analysis suffers from several puzzling features [25]. From the viewpoint of the electronic structure of the active metal ion, N_2O catalytic decomposition can be interpreted as follows [14]: in the course of the adsorption and activation of the N_2O molecule according to (R1), the active site acts as an electron donor into the N_2O antibonding orbital and, consequently, the electron density around the active site represents a decisive factor. The anion vacancies can act as active sites for N_2O chemisorption, too [7,16,26,27]. The oxygen desorption from the catalyst surface (reduction) is connected with an electron transfer back to the active site, the capability of the active site to accept electrons being a significant factor for the rate of (R3) step. Thus, the adsorption of N_2O and the desorption of O_2 are relatively easy in the presence of metals having mixed valence states. Mn^{3+}/Mn^{4+} and Cu^{2+}/Cu^{3+} couples were reported as active sites for the N_2O decomposition [7].

The possible application of mixed oxide based catalysts prepared by thermal treatment of hydrotalcite-like compounds (HTL) has been investigated recently [16,26,28–46] and these catalysts were reported as very active in N_2O decomposition. Hydrotalcite-like compounds, a class of layered double hydroxides, consist of positively charged metal hydroxide layers separated by anions and water molecules. Their chemical composition can be represented by the general formula $[M^{II}_{1-x}M^{III}_x(OH)_2]^{x+}[A^{n-}_{x/n} \cdot yH_2O]^{x-}$, where M^{II} and M^{III} are divalent and trivalent metal cations, A^{n-} is an n-valent anion, and x assumes usual values between 0.25 and 0.33 [47].

Although a great number of studies related to N_2O catalytic decomposition over calcined hydrotalcites has been published as yet, most of them deal with the catalytic performance of catalysts prepared from hydrotalcite precursors containing only single transition metal in the structure. In this study, not only the catalysts prepared by thermal treatment of hydrotalcite precursors with one transition metal, but also the synergic effect of two transition metals on the catalytic activity in N_2O decomposition will be studied. Nickel and manganese were selected as the transition metals, since the calcined Ni-Al hydrotalcite is known as an active catalyst for N_2O decomposition [31]. Manganese can exist in multiple oxidation states and the catalytic activity for N_2O decomposition over manganese oxides and some Mn containing mixed oxides was reported earlier [9,48]. The catalytic decomposition of N_2O over calcined hydrotalcite-like compounds containing manganese has been reported only in our recent work [49], where Co- and Mn-containing mixed oxides were examined.

We set out the following aims of the present paper: (i) preparation and characterization of two catalytic systems (calcined Ni-(Mg)-Al and Ni-(Mg)-Mn hydrotalcite-like compounds), (ii) their screening for the N_2O decomposition and the discussion of a mutual synergic effect of two transition metals (Ni and Mn) present in the catalysts on their activity in N_2O decomposition and (iii) finding a correlation among some characteristics of the prepared catalysts and their catalytic activity for the N_2O decomposition. The effect of oxygen and NO_2 inhibition is also studied.

2. Experimental methods

2.1. Preparation and characterization of the catalysts

The Ni-Mg-Al hydrotalcite-like precursors with Ni:Mg:Al molar ratios of 4:0:2, 3:1:2, 2:2:2 and 0:4:2 (assigned as Ni4Al2-HT, Ni3MgAl2-HT, Ni2Mg2Al2-HT and Mg4Al2-HT, respectively) and Ni-Mg-Mn hydrotalcite-like precursors with Ni:Mg:Mn molar ratio of 4:0:2, 2:2:2 and 0:4:2 (assigned as Ni4Mn2-HT, Ni2Mg2Mn2-HT and Mg4Mn2-HT, respectively) were prepared by coprecipitation. An aqueous solution (450 ml) containing appropriate amounts of $Ni(NO_3)_2{\cdot}6H_2O$, $Mg(NO_3)_2{\cdot}6H_2O$ and $Al(NO_3)_3{\cdot}9H_2O$ or $Mn(NO_3)_2{\cdot}4H_2O$ with total metal ion concentration of 1.0 mol l^{-1} was added dropwise with vigorous stirring into 200 ml of 0.5 M Na_2CO_3 solution. The mixing took about 1 h. During synthesis, the temperature was maintained at 25 °C and pH adjusted at ~10 by a simultaneous addition of the 3 M NaOH solution. The resulting suspension was stirred at 25 °C for additional 18 h. The product was filtered off, washed several times with distilled water and dried overnight at 60 °C in air. The dried precursors were formed into pellets of 3 mm in diameter, dried at 130 °C for 4 h and then calcined for 4 h at 500 °C in air. The calcined samples were crushed and the fraction of particle size 0.160–0.315 mm was used for catalytic measurements. The catalysts were signed as Ni4Al2,

Ni3MgAl2, Ni2Mg2Al2, Mg4Al2, Ni4Mn2, Ni2Mg2Mn2 and Mg4Mn2.

The thermal analysis was carried out using Netzsch STA 409 instrument. The heating rate of 10 °C min^{-1} in air with flow rate of 75 ml min^{-1} and 50 mg sample were used.

The powder X-ray diffraction (XRD) patterns were recorded using XRD powder diffractometer INEL CPS 120 equipped with a curved position-sensitive detector CPS120 (120° 2θ), reflection mode with a germanium monochromator (to produce Cu Kα_1 radiation). Silicon powder was used as standard reference material for calibration of CPS detector. Samples were pressed into the flat rotation holder and examined under the same experimental conditions during 2000 s. The applied voltage and current were 25 kV and 15 mA, respectively.

The surface area of the catalysts was measured by nitrogen adsorption at 77 K and evaluated by one point BET method. Prior to each measurement, the samples of prepared catalysts were heated 0.5 h at 350 °C.

The temperature-programmed reduction (TPR) measurements were carried out in an apparatus where a hydrogen–nitrogen mixture (10 mol% H_2) was used to reduce the sample (50 mg) at a flow rate of 40 ml min^{-1}. The temperature was linearly raised at a rate of 20 °C min^{-1} up to 850 °C. After freezing out the arising water at −76 °C, the gas mixture was analyzed by a thermal conductivity detector.

Temperature-programmed desorption (TPD) of CO_2 was carried out on a catalyst sample of 0.05 g under helium as carrier gas (flow rate 15 cm^3 h^{-1}). Prior to CO_2 adsorption, all catalysts were heated up to 450 °C. Then, 10 doses (840 μl each) of CO_2 were injected into the helium stream at 30 °C and the desorption of CO_2 was invoked by heating (20 °C min^{-1}) up to the final temperature of 450 °C. The Origin program (Microcal Software, Inc., MA, USA) was applied to analyze all desorption peaks.

2.2. Catalytic testing for nitrous oxide decomposition

The nitrous oxide decomposition reaction was performed in fixed-bed stainless steel reactor of 5 mm internal diameter (i.d.) in the temperature range 300–450 °C. It was verified that stainless steel did not contribute to the catalyst performance at given reaction conditions. The total flow rate was maintained between 30 and 160 cm^3 min^{-1} NTP (273 K, 101,325 Pa). The catalyst bed contained 0.1 or 0.2 g sample of the catalyst. The inlet content of N_2O was 0.05–0.15 mol% balanced by helium. Oxygen (0.5–5 mol%) and nitrogen dioxide (0.04–0.15 mol%) were added in some runs to evaluate the performance under these conditions. A temperature-controlled furnace was used for the reactor heating. Prior to each run, the catalysts were heated by the rate 10 °C min^{-1} up to 450 °C in a helium flow of 50 cm^3 min^{-1} and the temperature was maintained for 1 h. After the pre-treatment, the feed mixture was passed over the catalyst and the reaction processed overnight. Then the conversion at 450 °C was measured and the temperature was decreased to the desired level. Generally, 1 h after a change of conditions, the nitrous oxide conversion level was constant and considered to attain a steady state. At least three analyses were averaged to get a single data point.

The gas chromatograph Hewlett Packard (model 5890, series II GC) equipped with the electron capture detector was used to analyze the nitrous oxide content in the gas. The data were acquired with HP Chemstation. The PoraPlot Q (30 m × 0.53 mm × 40 μm) column and an electron capture detector operating in overheating mode (330 °C) were used in the chromatographic analysis. The two-points calibration with calibration gases (0.007 and 0.1 mol% N_2O) was performed before and after each experimental run.

The application of the experimental tests and the criteria to check the presence of mass and heat transport limitations in the reactor revealed that these restraints were absent [50].

3. Results and discussion

3.1. Characterization of catalysts

The results of the elemental chemical analysis of the dried hydrotalcite-like precursors are presented in Table 1. The content of the metal cations in the dried products correspond roughly to the respective molar ratios in the nitrate solutions used in coprecipitation. The precursors contained a small amount of Na cations. Higher amounts of Na^+ in the Ni2Mg2Mn2 and Mg4Mn2 precursors were probably caused by insufficient washing.

The DTA curves of the prepared precursors showed two endothermic effects characteristic for the hydrotalcite-like compounds. The first endothermic effect was ascribed to the release of interlayer water (dehydration) while the second one to the sample decomposition including dehydroxylation of the hydroxide layers and the decomposition of interlayer carbonate. The dehydration and decomposition temperatures of the prepared

Table 1
The chemical composition of the hydrotalcite-like precursors dried at 60 °C

Precursor	Ni (wt.%)	Mn (wt.%)	Mg (wt.%)	Al (wt.%)	Na (wt.%)	Molar ratio Ni:Mg:M^{III}
Ni4Al2-HT	35.9	0	0	8.39	0.007	1:0:0.508
Ni3MgAl2-HT	27.0	0	3.86	8.43	0.002	1:0.346:0.678
Ni2Mg2Al2-HT	19.2	0	8.44	9.07	0.002	1:1.061:1.030
Mg4Al2-HT	0	0	15.90	9.10	0.027	0:1:0.526
Ni4Mn2-HT	33.0	16.11	0	0	0.007	1:0:0.522
Ni2Mg2Mn2-HT	19.5	16.58	7.12	0	0.140	1:0.882:0.909
Mg4Mn2-HT	0	22.00	19.42	0	0.378	0:1:0.501

Table 2
The dehydration and decomposition temperatures of the prepared hydrotalcite-like precursors (the temperatures of the first and second endothermic minima observed in DTA curves)

Precursor	Dehydration temperature (°C)	Decomposition temperature (°C)
Ni4Al2-HT	120	360
Ni3MgAl2-HT	130	390
Ni2Mg2Al2-HT	140	390
Mg4Al2-HT	215	400
Ni4Mn2-HT	160	245
Ni2Mg2Mn2-HT	165	270
Mg4Mn2-HT	160	295

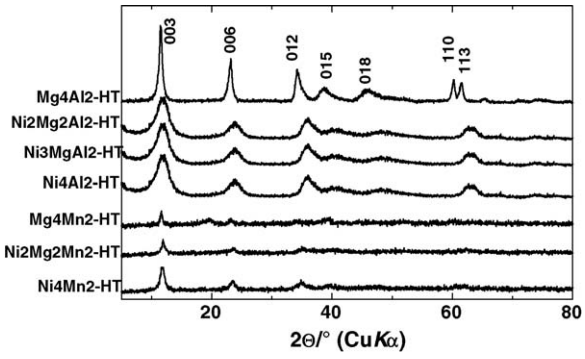

Fig. 1. X-ray powder diffraction patterns of the prepared hydrotalcite-like compounds.

precursors corresponding to the endothermic minima on measured DTA curves are presented in Table 2. A higher content of the transition metals (Ni and Mn) caused a decrease of the thermal stability of the prepared precursors.

Only a well-crystalline hydrotalcite-like phase was found in the powder XRD patterns of the dried precursors (Fig. 1) except for Ni4Mn2 and Mg4Mn2 samples, where trace amounts of $MnCO_3$ (rhodochrosite) were detected. The powder XRD patterns of the prepared catalysts are presented in Fig. 2. The broad diffraction lines corresponding to MgO (periclase) and NiO (bunsenite) were detected in the calcined Mg4Al2 and Ni4Al2

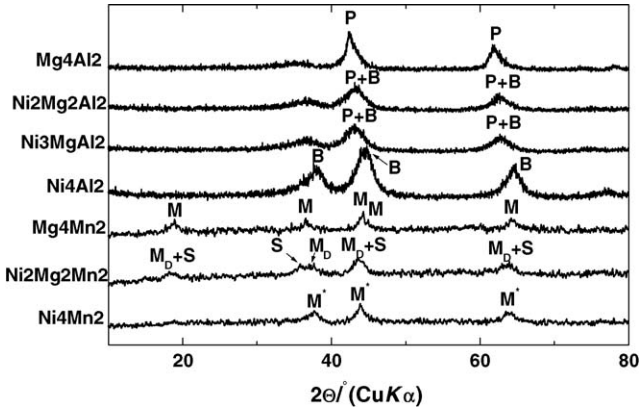

Fig. 2. X-ray powder diffraction patterns of the hydrotalcite-like compounds calcined at 500 °C. P-MgO (periclase), B-NiO (bunsenite), M-Mg_6MnO_8 (murdochite), M_D-$(Ni,Mg)_6MnO_8$ (disordered murdochite), S-$Ni_xMg_yMn_zO_4$ spinel, M^*-Ni_6MnO_8 (murdochite).

Table 3
The average valence of Mn in the mixed oxides prepared by calcination of Mn-containing hydrotalcite-like precursors at 500 °C

Calcination temperature (°C)	Mn valence		
	Ni4Mn2	Ni2Mg2Mn2	Mg4Mn2
300	4.00	3.93	3.72
400	4.00	4.00	3.78
500	4.00	4.00	3.75
600	3.85	3.94	3.70

samples, respectively. The mixed oxide Ni_6MnO_8 with murdochite structure was found in the calcined Ni4Mn2 sample. This oxide is formed at about 300 °C and it was detected in calcined products obtained at temperatures up to ca. 800 °C. The other oxide containing also the tetravalent manganese, $NiMnO_3$ with ilmenite structure, was found when the Ni4Mn2 hydrotalcite was heated at 500–700 °C [51]. During the heating of Ni2Mg2Mn2 precursor, the $Ni_xMg_yMn_zO_4$ spinel and cubic $(Ni,Mg,Mn^{IV})O$ oxide were detected in the powder XRD pattern of the samples calcined at 400–600 °C. The latter oxide was assigned to a disordered murdochite, M_D, taking into account its too low lattice parameter, resembling rather *a*/2 of Mg-doped murdochite $(Ni,Mg)_6MnO_8$ than *a* of Mg-doped bunsenite (Ni,Mg)O (the term 'disordered' refers to a disordered cation position in the parent bunsenite structure) [50]. The mixed oxide with murdochite structure, Mg_6MnO_8, was detected also in the powder XRD pattern of the Mg4Mn2 catalyst prepared at 500 °C. The presence of Mn^{IV}-containing oxides in the products obtained during heating of Ni-Mg-Mn and Ni-Mn samples was confirmed also by the elemental and redox analysis (iodometry) of the calcined samples (Table 3). By contrast, the presence of Mn in lower oxidation states could be expected on the basis of the average value of Mn valence in the Mg4Mn2 sample.

The surface area of the prepared catalysts increases from 70 $m^2\,g^{-1}$ for Ni4Mn2 to 298 $m^2\,g^{-1}$ for Mg4Al2 (Table 4). In principle, the Ni-(Mg)-Al catalytic system shows a higher surface area than the Ni-(Mg)-Mn system. The results proved increasing values of surface area with decreasing amount of nickel, especially in Ni-(Mg)-Al systems. Also Pérez-Ramírez et al. [39] published a decrease of the surface area with the decreasing Co content in the Co-Mg-Al calcined hydrotalcite.

As the sufficiently large surface area is important for the heterogeneous catalysis, an effort was exerted to find a reason for the specific surface differences in the respective catalyst series, Ni-(Mg)-Al and Ni-(Mg)-Mn. The relation between the temperatures of thermal decomposition (T °C) and the surface areas of the prepared catalysts calcined at 500 °C ($S_{BET,500\,°C}$) can be described by an exponential regression equation: $S_{BET} = 6.27\,e^{0.0093T}$ with the correlation coefficient $R^2 = 0.92$ (Fig. 3). The obtained correlation can be explained as in terms of an enhanced release of water and CO_2 from the crystal structure with increasing temperature causing an increase of the surface area of the calcined powders. The maximum value of the surface area can be achieved in the vicinity of decomposition temperature. A progressive increase in the calcination temperature leads to a consecutive crystallization of the arising oxidic

Table 4
The specific surface area of the prepared catalysts, H_2 consumption, the amount of desorbed CO_2 in the temperature range 350–450 °C and N_2O decomposition rate constants k (at 400 °C) determined from the experiments in inert gas using the first order kinetic law

Catalyst	S_{BET}[a] ($m^2\ g^{-1}$)	mmol $CO_2\ g^{-1}$ (350–450 °C)	mmol $H_2\ g^{-1}$ (350–450 °C)	k (400 °C)[b]/10^{-12} (mol $m^{-2}\ s^{-1}\ Pa^{-1}$)	k (400 °C)[b]/10^{-9} (mol $g^{-1}\ s^{-1}\ Pa^{-1}$)
Ni4Al2	190	0.051	1.190	16.5	3.135
Ni3MgAl2	209	0.074	0.375	7.8	1.640
Ni2Mg2Al2	245	0.076	0.400	1.8	0.441
Mg4Al2	298	0.107	0.100	0.4	0.119
Ni4Mn2	70	0.042	8.190	2.8	0.196
Ni2Mg2Mn2	86	0.046	1.600	1.7	0.146
Mg4Mn2	70	0.047	3.880	14.2	1.562

[a] Specific surface area of extrudates calcined at 500 °C.
[b] Rate constants of N_2O decomposition determined using first order kinetic law, inlet: 0.1 mol% N_2O in He.

phases and to a decrease of the surface area. As all our catalysts were calcined at the same calcination temperature (500 °C), the highest surface areas were reached with the compounds exhibiting decomposition temperatures near 500 °C. On the other hand, the compounds decomposing at much lower temperatures than the catalyst calcination temperature showed substantially lower surface areas.

The temperature-programmed reduction patterns (Fig. 4) showed different reduction behavior for the catalyst series containing Al and Mn. In the case of Ni4Al2 catalyst, the TPR pattern shows a broad peak with a maximum around 530 °C, which is attributed to the reduction of $Ni^{2+} \rightarrow Ni^0$. This temperature is significantly higher than that of the bulk NiO (330 °C) [52], but it is known that NiO obtained by calcinations of Ni-Al hydrotalcite precursors is more difficult to reduce than the bulk NiO [53]. According to the literature data [54–57], the oxidic forms with a spinel-type local order are responsible for hindering the reduction of NiO in the calcined Ni-Al hydrotalcite. Compared to Ni4Al2 catalyst, the TPR profiles of the Ni-Mg-Al catalysts show that the presence of Mg caused a broadening of the reduction peaks and a shift of the reduction temperatures of Ni^{2+} species towards higher values, which is well documented in the literature [58,59]. This shift is associated with the formation of a NiO–MgO solid solution in which Ni^{2+} ions are stabilized by the MgO-type matrix against reduction and sintering. The first low temperature maximum at Ni3MgAl and Ni2Mg2Al2 samples could correspond to the reduction of a physically adsorbed Ni-oxide–hydroxide phase [60]. The TPR of Mg4Mn2 is similar to the reduction of MnO_x mentioned in the literature [61–63] and corresponds to the reduction process $Mn^{4+} \rightarrow Mn^{3+,4+} \rightarrow Mn^{2+}$. The specific surface area and the crystallinity of the sample control the temperatures of the individual reduction steps [64].

The TPR profiles of our catalysts obtained within the temperature range 20–800 °C were analyzed and the amount of oxides reducible in the temperature region covering the N_2O decomposition reaction (350–450 °C) was evaluated (Table 4). In the Ni-(Mg)-Al system, this amount of reducible species decreased with decreasing amount of Ni in the catalysts. A different dependence was found for the amount of reducible components in Ni-(Mg)-Mn system: the amount of reducible components increases

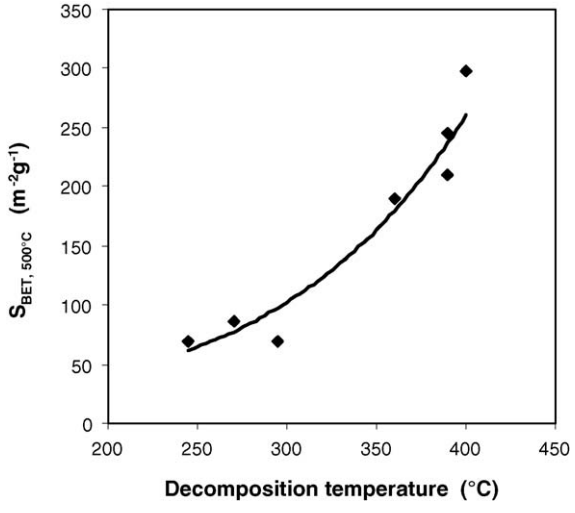

Fig. 3. Relation between thermal decomposition temperatures of the hydrotalcite-like compounds determined from DTA (an extreme in the second peak) and S_{BET} area measured after their calcination at 500 °C.

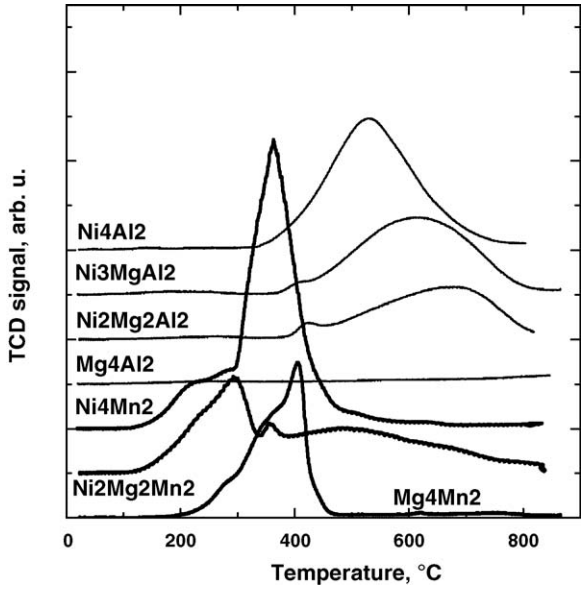

Fig. 4. TPR curves of the Ni-(Mg)-Al and Ni-(Mg)-Mn catalytic systems prepared by calcination (500 °C) of corresponding hydrotalcite-like compounds.

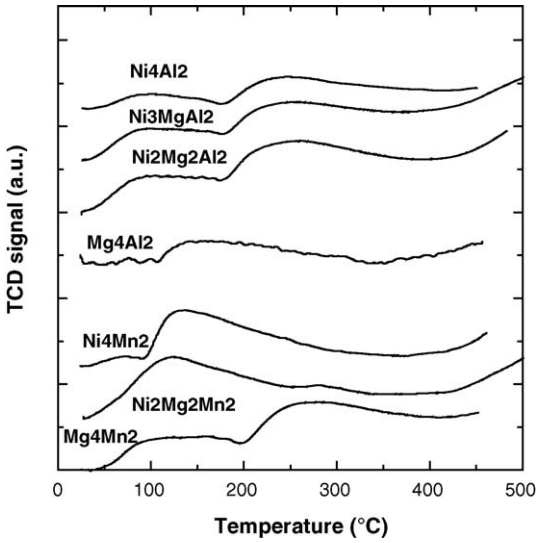

Fig. 5. TPD CO_2 curves of the Ni-(Mg)-Al and Ni-(Mg)-Mn catalytic systems prepared by calcination (500 °C) of corresponding hydrotalcite-like compounds.

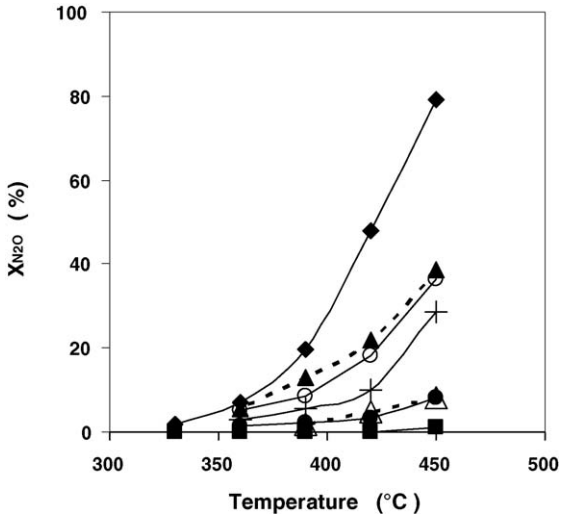

Fig. 7. Conversions of N_2O as a function of temperature. (♦) Ni4Al2, (▲) Mg4Mn2, (◯) Ni3MgAl2, (+) Ni2Mg2Al2, (●) Ni4Mn2, (△) Ni2Mg2Mn2 and (■) Mg4Al2. Conditions: 0.1 g sample, 100 cm^3 min^{-1} and 0.1 mol% N_2O.

in the order Ni2Mg2Mn2 < Mg4Mn2 < Ni4Mn2. The Ni4Mn2 catalyst exhibited the highest amount of reducible compounds of all catalysts.

The desorption of CO_2 from the calcined hydrotalcite-like compounds in the temperature range 20–450 °C can be seen in Fig. 5. The amounts of CO_2 (Table 4) desorbing in the reaction temperature range (350–450 °C) were calculated from the TPD curves. The relation of both, the amount of hydrogen consumed and the amount of CO_2 evaluated for the temperature region 350–450 °C can be seen in Fig. 6. An exponential decay of the amount of CO_2 (corresponding to strong basic sites) with the increasing catalyst reducibility was observed in this set of catalysts.

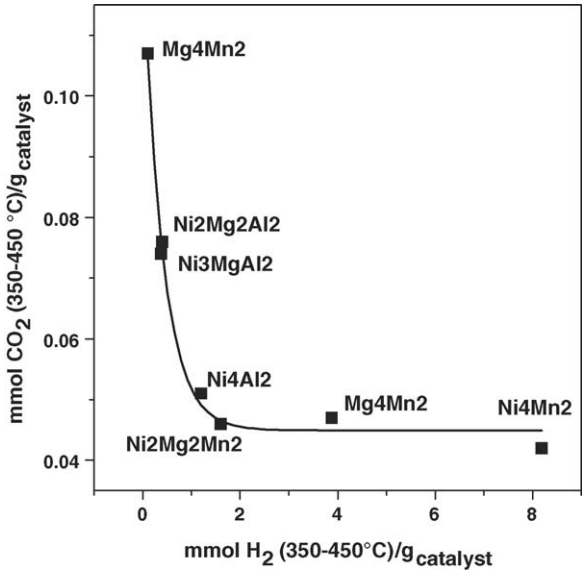

Fig. 6. Correlation of the catalyst reducibility (the amount of hydrogen consumed in the temperature range 350–450 °C) and the catalyst basicity (the amount of CO_2 desorbed between 350 and 450 °C), correlation equation $y = 0.07882 \exp(-x/0.4084) + 0.04491$, $R^2 = 0.99$.

3.2. Catalytic activity in N_2O decomposition

The nitrous oxide conversion as a function of reaction temperature is given in Fig. 7. In the temperature range studied, the Mg4Al2 system was completely inactive as it has been previously documented [29]. The substitution of Mg^{2+} for Ni^{2+} resulted in an increased catalytic activity in the order: Mg4Al2 < Ni2Mg2Al2 < Ni3MgAl2 < Ni4Al2. The highest nitrous oxide conversion, 79%, was reached over the Ni4Al2 catalyst. The substitution of Al^{3+} for Mn^{3+} in Mg4Al2 catalyst (Mg4Mn2 catalyst) caused also an increase in catalytic activity (39% N_2O conversion), but the substitution Mg^{2+} for Ni^{2+} mentioned before (Ni4Al2 catalyst) resulted in much higher increase in catalyst activity. The substitution of both, Mg and Al in Mg4Al2 sample, by transition metals Ni and Mn, respectively (Ni2Mg2Mn2 and Ni4Mn2), resulted, compared to Ni4Al2, in a sharp decrease in catalytic activity, both catalysts were thus found to be relatively inactive.

The detailed kinetic analysis with the most active catalyst Ni4Al2 revealed that the kinetic data are well described (Fig. 8) by first order rate law $-(\mathrm{d}p_{N_2O}/\mathrm{d}t) = k \cdot p_{N_2O}$ corresponding to no oxygen inhibition, similar to what Kannan [31] and Chang et al. [65] have found. The kinetic parameters $E_a = 112$ kJ mol^{-1} and $\ln k_0 = 14.5$ were evaluated by the method of initial reaction rates.

The manganese-containing catalysts Ni-(Mg)-Mn exhibited three to four times lower specific surface areas than the Ni-(Mg)-Al catalysts. To find out whether the lower surface area of Ni-(Mg)-Mn catalysts (connected with generally lower thermal stability of their hydrotalcite-like precursors as determined from DTA) is the only reason for the low catalytic activity, the reaction rate constants k (mol g^{-1} s^{-1} Pa^{-1}) were evaluated according to the first order rate law for all catalysts and related to a unit surface area (Table 4). The activity of the catalysts expressed as a kinetic constant k (mol m^{-2} s^{-1} Pa^{-1}) decreases in the order: Ni4Al2 > Mg4Mn2 > Ni3MgAl2 > Ni4Mn2 ≥ Ni2Mg2Al2 ≥

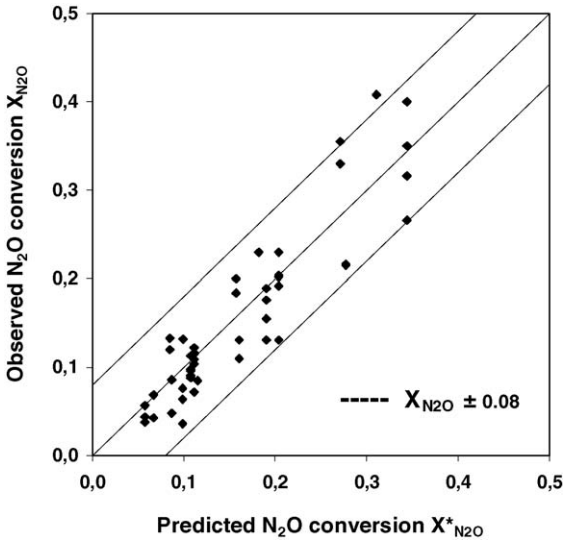

Fig. 8. Comparison of experimental N_2O conversion (X_{N_2O}) obtained in oxygen-free helium as feed gas and that one determined according to first order kinetic law ($X^*_{N_2O}$). Conditions: 360–400 °C, 0.05–0.15 mol% N_2O and Ni4Al2 catalyst.

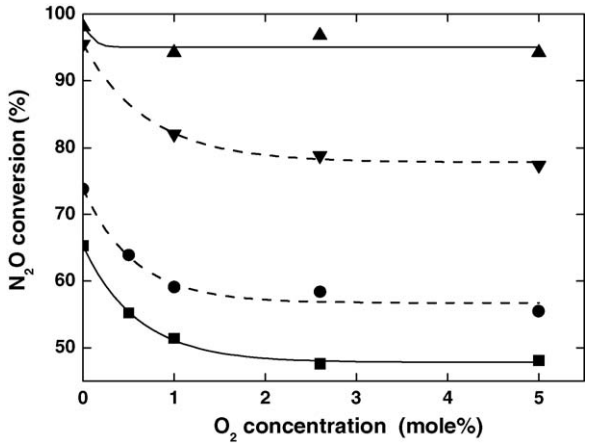

Fig. 9. Conversion of N_2O as a function of oxygen concentration. (▲) Ni3MgAl2, (▼) Ni4Al2, (●) Mg4Mn2 and (■) Ni2Mg2Al2. Conditions: 450 °C, 0.2 g sample, 50 cm^3 min^{-1} and 0.1 mol% N_2O.

Ni2Mg2Mn2 ≥ Mg4Al2. Evidently, a combination of Ni and Mn in the hydrotalcite based catalysts, compared to the catalysts containing only one of these metals (Ni4Al2 or Mg4Mn2), caused a decrease in catalytic activity for N_2O decomposition, although the order of activities (mol m^{-2} s^{-1} Pa^{-1}) slightly changed (k for Ni4Al2 is closer to Mg4Mn2).

The selected active catalysts were also tested in the presence of oxygen and nitrogen dioxide in the inlet reaction mixture. The experiments with a reaction mixture gradually enriched by oxygen showed that the N_2O conversion decreased only to a certain oxygen concentration level (approximately 3 mol% O_2); while at higher oxygen concentrations the reaction rate became independent of the oxygen concentration (Fig. 9). A similar influence of oxygen on the N_2O decomposition rate was observed over platinum [17] and some zeolite catalysts [66]. This experimental observation can be accounted for by a slow-down of the reaction step (R1) due to an oxygen adsorption on the active sites of the catalytic surface, which demands free active sites, whereas (R3) step does not. When the surface is totally covered by the adsorbed oxygen, the N_2O decomposition proceeds according to Eq. (R3) only and the rate of the process is independent of the additional increase of the oxygen concentration. The kinetic experiments performed at higher oxygen concentrations (when the reaction rate is independent of oxygen concentration) showed that data are again well correlated by the first order rate law as was also proposed by Golodets [14] and Chang et al. [65]. The addition of NO_2 to the reaction mixture caused a further decrease in N_2O conversion, probably resulting from a competitive adsorption of NO_2 on the active sites. The N_2O conversions measured in the presence of both O_2 and NO_2 and rate constants k^* evaluated according to the first order kinetic equation (for compositions of initial reaction mixtures: 0.1 mol% N_2O and 5 mol% O_2 in He) are summarized in Table 5.

4. Discussion

It follows from the results mentioned above that the catalytic activity of the calcined Ni-(Mg)-Al hydrotalcite-like compounds in N_2O decomposition expressed as both conversion and k (mol m^{-2} s^{-1} Pa^{-1}) decreases with the increasing amount of Mg in the catalysts, while the activity of the calcined Ni-(Mg)-Mn hydrotalcite-like compound shows, by contrast, no such trend. This finding can be linked to a number of active sites capable to take part in the oxidation–reduction processes, detectable as the amounts of reducible components (mmol H_2 g^{-1}) determined in the temperature range 350–450 °C, i.e. in the range in which the catalytic reaction takes place. With the increasing amount of Mg in the Ni-(Mg)-Al system the number of reducible compounds

Table 5
N_2O conversions and kinetic constants k^* for N_2O decomposition at 0.1 mol% N_2O and 5 mol% O_2 determined using first order kinetic

Catalyst	N_2O conversion (%)	k^* (400 °C)/10^{-10} (mol g^{-1} s^{-1} Pa^{-1})	k^* (400 °C)/10^{-12} (mol m^{-2} s^{-1} Pa^{-1})
Ni4Al2	99[a] (94[b], 57[c])	23.7	12.6
Ni3MgAl2	97[a] (85[b], 26[c])	14.4	6.9
Ni2Mg2Al2	49[a] (34[b], 8[c])	3.9	1.6
Mg4Mn2	53[a] (36[b], 10[c])	6.2	8.9

[a] Test conditions: 0.1 mol% N_2O in He, m = 0.2 g, flow rate 100 cm^3 min^{-1}, 450 °C.
[b] With 5 mol% O_2.
[c] With 5 mol% O_2 and 0.02 mol% NO_2.

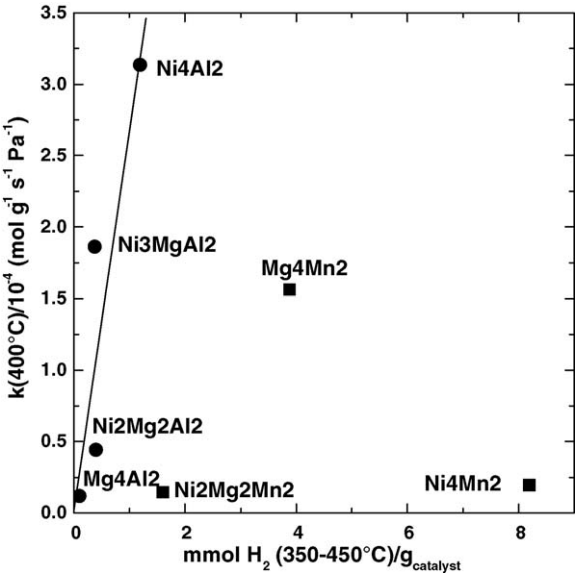

Fig. 10. Correlation of the rate constants k (determined by first order kinetic from experiments in He) and the amount of oxides reducible in the temperature region covering reaction temperature 350–450 °C.

strongly decreases, but a different dependence was found for the number of reducible components in Ni-(Mg)-Mn system: neither increasing nor decreasing tendency in reducibility with the amount of Mg in the catalysts was found, however, the number of reducible components increases with the amount of Ni in the order Ni2Mg2Mn2 < Mg4Mn2 < Ni4Mn2 (Fig. 6).

The observed different dependencies of activity in both systems on the amounts of the reducible compounds are in relation to a hypothetical mechanism of N_2O decomposition, in which an electron transfer from an active site and a splitting of N–O bond is the primary step and the adsorbed oxygen remains on the catalyst surface. The adsorbed oxygen is then desorbed in the next step, and the electron is transferred back to the active site. This step, desorption of oxygen, is concluded to be the most difficult step of the reaction over many catalysts [14,20,21,66,67].

Our results obtained over the calcined Mg4Al2 catalyst show that activity of the catalyst is negligible when the catalyst reduction does not occur in the reaction temperature range. Similarly, a very low N_2O conversion in the temperature range 350–450 °C was observed over the calcined Mg-Cr hydrotalcite-like compound [33] and a negligible amount of reducible components in this temperature range was observed by Rives et al. [68]. We can state that the first assumption for obtaining an active N_2O decomposition catalyst is the presence of components reducible in the reaction temperature range. In the series of the Ni-(Mg)-Al catalysts, the catalytic activity increases with increasing amount of reducible components, i.e. with increasing amount of Ni in the catalyst (Fig. 10). Similar results were observed for various solid solutions containing different transition metal ions dispersed in an inert matrix. As the metal concentration is increased, the electron transfer within the bulk and the surface becomes increasingly efficient and hence, the adsorption process (R1) is facilitated [32]. When the amount of reducible components is higher than an optimum value (in case of the Ni-(Mg)-Mn system the Mg4Mn2 catalyst is the most active and it corresponds to an optimal amount of the reducible components) then the ability of the catalysts to catalyze the N_2O decomposition decreases (Fig. 10). This could be due to an inappropriate geometric arrangement of the active sites on the catalyst surface or a too strong oxygen bond to the surface and consequently a slow O_2 desorption.

Although a correlation between the catalysts reducibility and the catalysts basicity was found (Fig. 6), no direct connection of the amount of strong basic sites and the catalytic activity was observed. It is thus considered that the catalyst basicity is probably not a key parameter for the catalytic activity. Alini et al. [33] came to similar results in the study of calcined Rh-Mg-Al hydrotalcite-like compounds and their effect on the N_2O decomposition. They observed that the changes in the Mg/Al ratio (i.e. basicity of the oxide matrix) did not cause any significant differences in the activity of the calcined hydrotalcite-based catalysts in the case when the amount of rhodium was the same. On the contrary, Tabata et al. [27] reported the catalytic activity of the murdochite type catalysts $(Mg_{6-x}Li_x)MnO_8$ during the decomposition of N_2O being increased with the increasing amount of Li (Li increases the number of oxygen vacancies acting as active sites). A better catalytic performance in the presence of a residual Na remaining as trace amounts after washing step was already published. A small but critical amount of activator metal is supposed to promote the decomposition of N_2O. The optimum content of Na (∼1 wt.%) was published [37]. The highest amount of sodium in our catalysts was found in the Mg4Mn2 sample (Table 1). Sodium in this catalyst can contribute to the high catalytic activity and to the high basicity as well (the amount of CO_2 desorbed from this catalyst in the range 350–450 °C related to surface area is the highest).

The amount of reducible components in the catalysts is evidently related to the oxidation state of the transition metal. It was found earlier that the transition metal oxidation state determines the electron donation properties and the activity in nitrous oxide decomposition [10]. It has been argued that from four manganese oxides, MnO, Mn_3O_4, Mn_2O_3 and MnO_2, the Mn_2O_3 oxide is the phase associated with the highest catalytic activity [48]. The studies of N_2O decomposition over Mn^{3+}/Mn^{4+} ions in very diluted ion concentrations dispersed in MgO matrix have revealed [2] that Mn^{3+} ions are more active than Mn^{4+} ions because the oxygen is held less strongly on the former ones. The d^4 configuration of Mn^{3+} is known to provoke a formation of two weaker bonds to the ligands in octahedrally coordinated complexes. Though the situation on the surface will differ from that encountered for a free coordination complex and the d^4 complex will therefore loose its optimum symmetry, these two bonds will still be weaker than those in the plane. It may be recalled that the d^4 configuration, together with d^9 configuration, shows a favorable contribution for a dissociation mechanism from the standpoint of the Crystal field stabilization energy [69]. It was supposed [70] that Mn^{3+} and Mn^{4+} cations in lanthanum strontium manganite do not act as individual active ions (the reason is their high concentration). They are likely a part of large clusters acting as electron donors or electron acceptors. The Mn^{3+}/Mn^{4+} redox couple (in the 1:1 ratio) possesses a capacity to facilitate

easy change transfers, and thus exhibits the maximum catalytic activity.

These findings correspond well with our experimental results: from all Mn containing catalysts only the Mg4Mn2 system showed a high activity for N_2O decomposition caused by the presence of manganese in lower oxidation state than Mn^{4+} as suggested by iodometry redox analysis (see Table 3). The Mn^{3+}/Mn^{4+} redox couple possibly acts as an active site in this catalyst. On the contrary, Ni2Mg2Mn2 and Ni4Mn2 catalysts contained almost all manganese in the Mn^{4+} oxidation state as was determined from redox analysis and therefore their activity for N_2O decomposition was lower.

It remains to discuss why nickel in Ni-(Mg)-Mn catalysts does not act as an active site, whereas in the Ni-(Mg)-Al catalysts does. Cimino et al. [71] found that Ni^{3+} ions are less active in decomposition of N_2O than Ni^{2+} cations. The reason for such a behavior is a stronger bonding of oxygen in the surface Ni^{3+}–O than Ni^{2+}–O complexes, which brings along a slower desorption of the adsorbed oxygen. For that reason, the oxidation state of nickel in both types of catalysts was compared. A careful investigation of the XPS spectra of the calcined Ni-Al hydrotalcite and the NiO and $NiAl_2O_4$ reference compounds was reported previously [72] revealing an oxidation state Ni^{2+} on the Ni4Al2 surface indicated by characteristic satellite lines in the spectrum. By contrast, in the Ni2Mg2Mn2 catalyst (exhibiting low catalytic activity), Ni^{3+} oxidation state of nickel was found as prevailing [73].

5. Conclusions

The combination of Ni and Mn in the hydrotalcite based catalysts caused a decrease in the catalytic activity for N_2O decomposition compared to the prepared catalysts containing only one of these metals. The manganese-containing catalysts Ni-(Mg)-Mn exhibit three to four times lower specific surface area than Ni-(Mg)-Al catalysts, this phenomenon being likely connected with a generally lower thermal stability of Ni-(Mg)-Mn hydrotalcite-like precursors. However, not only the lower specific surface area is the reason for the inferior catalytic performance of Ni-(Mg)-Mn catalyst series. The activities of catalysts are also related to both the oxidation state of transition metals Ni and Mn and the amount of reducible components in the temperature range where the N_2O decomposition is taking place. The catalysts active in N_2O decomposition should have a certain optimum amount of the components reducible in the temperature range 350–450 °C. The oxidation states of nickel and manganese are also important for achievement of a high catalytic activity. The best catalysts are those with manganese and nickel in Ni^{2+} and Mn^{3+} oxidation states, respectively, while those with manganese and nickel in Mn^{4+} and Ni^{3+} are less active. It follows from the kinetic results that the reaction rate of N_2O decomposition in He is described by first order rate law. The presence of oxygen in the inlet reaction mixture was found to cause an inhibition up to the concentration of 3 mol% O_2 only, while at higher oxygen concentrations the N_2O conversion is nearly constant. A strong inhibition was observed when nitrogen dioxide was present in the inlet reaction mixture.

Acknowledgements

Thanks are due to B. Smetana for the help with the catalytic N_2O decomposition experiments. This work was supported by the Grant Agency of the Czech Republic (Grants No. 106/05/0366 and No. 104/04/2116) and by the Czech Ministry of Education, Youth and Sports (Research Projects No. CEZ: MSM 6046137302 and 6198910016).

References

[1] F.S. Stone, J. Solid State Chem. 12 (1975) 271.
[2] A. Cimino, V. Indovina, J. Catal. 17 (1970) 54.
[3] C. Angeletti, F. Pepe, P. Porta, J. Chem. Soc. Faraday Trans. 1 (1978) 1595.
[4] C.S. Swamy, J. Christopher, Catal. Rev.-Sci. Eng. 34 (1992) 409.
[5] K.V. Ramanujachary, N. Kameswari, C.S. Swamy, J. Catal. 86 (1984) 121.
[6] J. Christopher, C.S. Swamy, J. Mol. Catal. 68 (1991) 199.
[7] J. Christopher, C.S. Swamy, J. Mol. Catal. 62 (1990) 69.
[8] A. Cimino, La Chimica e L'Índustria 56 (1974) 27.
[9] J. Wang, H. Yasuda, K. Inumaru, M. Misono, Bull. Chem. Soc. Jpn. 68 (1995) 1226.
[10] F. Kapteijn, J. Rodriguez-Mirasol, J.A. Moulijn, Appl. Catal. B 9 (1996) 25.
[11] J. Pérez-Ramírez, F. Kapteijn, G. Mul, X. Xu, J.A. Moulijn, Catal. Today 76 (2002) 55.
[12] C.M. Fu, V.N. Korchak, W. Keith Hall, J. Catal. 68 (1981) 166.
[13] E.R.S. Winter, J. Catal. 34 (1974) 431.
[14] G.I. Golodets, Stud. Surf. Sci. Catal. 15 (1983) 2001.
[15] K. Li, X.F. Wang, H.C. Zeng, Trans IchemE 75A (1997) 807.
[16] M.C. Román-Martínez, F. Kapteijn, D. Cazorla-Amorós, J. Pérez-Ramírez, J.A. Moulijn, Appl. Catal. A 225 (2002) 87.
[17] L. Riekert, D. Menzel, M. Staib, Proceedings of the Third International Congress on Catalysis, vol. 1, North-Holland Publ. Co., Amsterdam, 1965, p. 387.
[18] H. Uetsuka, K. Aoyagi, S. Tanaka, K. Yuzaki, S. Ito, S. Kameoka, K. Kunimori, Catal. Lett. 66 (2000) 87.
[19] H. Dandl, G. Emig, Appl. Catal. 168 (1998) 261.
[20] T.M. Miller, V.H. Grassian, Catal. Lett. 46 (1997) 213.
[21] J. Pérez-Ramírez, F. Kapteijn, G. Mul, J.A. Moulijn, J. Catal. 2008 (2002) 211.
[22] A.K. Vijh, J. Catal. 31 (1973) 51.
[23] P. Sabatier, Ber. 44 (1911) 2001.
[24] A.A. Balandin, Adv. Catal. 10 (1958) 120.
[25] Z. Knor, Appl. Catal. A 245 (2003) 185.
[26] J. Pérez-Ramírez, F. Kapteijn, J.A. Moulijn, Appl. Catal. B 23 (1999) 59.
[27] K. Tabata, T. Karasuda, E. Suzuki, J. Mater. Sci. 35 (2000) 4031.
[28] S. Kannan, C.S. Swamy, Catal. Today 53 (1999) 25.
[29] J.N. Armor, T.A. Braymer, T.S. Farris, Y. Li, F.P. Petrocelli, E.L. Weist, S. Kannan, C.S. Swamy, Appl. Catal. B 7 (1996) 397.
[30] C.S. Swamy, S. Kannan, Y. Li, J.N. Armor, T.A. Brayner, US Patent 5 407 652 (1995), to Engelhard Corporation.
[31] S. Kannan, Appl. Clay Sci. 13 (1998) 347.
[32] P. Kustrowski, L. Chmielarz, A. Rafalska-Lasocha, B. Dudek, A. Wegrzyn, R. Dziembaj, Przem. Chem. 82 (8–9) (2003) 732.
[33] S. Alini, F. Basile, A. Bologna, T. Montanari, A. Vaccari, in: E. Gaigneaux (Ed.), Studies in Surface Science and Catalysis, vol. 143, Elsevier Science, 2002, p. 131.
[34] S. Kannan, C.S. Swamy, Appl. Catal. B 3 (1994) 109.
[35] J. Pérez-Ramírez, F. Kaptejn, J.A. Moulijn, Catal. Lett. 60 (1999) 133.
[36] R.S. Drago, K. Jurczyk, US Patent 5 705 136 (1998), to University of Florida Research.
[37] T.S. Farris, Z. Li, J.N. Armor, T.A. Braymer, US Patent 5 472 677 (1995), to Engelhard Corporation.

[38] R.S. Drago, K. Jurczyk, N. Kob, Appl. Catal. B 13 (1997) 69.
[39] J. Pérez-Ramírez, G. Mul, X. Xu, F. Kapteijn, J.A. Moulijn, in: A. Corma, F.V. Melo, S. Mendioroz, J.L.G. Fierro (Eds.), Studies in Surface Science and Catalysis, 130, Elsevier Science, 2000, p. 1445.
[40] W. Bo, W. Shugin, Z. Yahui, Spectrosc. Lett. 30 (6) (1997) 1165.
[41] J. Oi, R. Tanaka, A. Obuchi, A. Ogata, G.R. Bamwenda, S. Kushiyama, Phys. Chem. 41 (1997) 119.
[42] J. Oi, A. Obuchi, A. Ogata, G.R. Bamwenda, H. Yagita, S. Kushiyama, K. Mizuno, Appl. Catal. B 12 (1997) 227.
[43] G. Centi, A. Galli, B. Montanari, S. Perathoner, A. Vaccari, Catal. Today 35 (1997) 113.
[44] J. Oi, A. Obuchi, A. Ogata, G.R. Bamwenda, R. Tanaka, T. Hibino, S. Kushiyama, Appl. Catal. B 13 (1997) 197.
[45] U. Chellam, Z.P. Xu, H.C. Zeng, Chem. Mater. 12 (2000) 650.
[46] J. Pérez-Ramírez, G. Mul, X. Xu, F. Kapteijn, J.A. Moulijn, J. Mater. Chem. 11 (2001) 821.
[47] F. Cavani, F. Trifiro, A. Vaccari, Catal. Today 11 (1996) 173.
[48] T. Yamashita, A. Vannice, J. Catal. 161 (1996) 254.
[49] L. Obalová, K. Jirátová, F. Kovanda, K. Pacultová, Z. Lacný, Z. Mikulová, Appl. Catal. B 60 (2005) 289.
[50] F. Kaptejn, J.A. Moulijn, in: G. Ertl, H. Knözinger, J. Weitkamp (Eds.), Handbook of Heterogeneous Catalysis, vol. 3, Wiley, Weinheim, 1996, p. 1359.
[51] F. Kovanda, T. Grygar, V. Dorničák, Solid State Sci. 5 (2003) 1019.
[52] S.D. Robertson, B.D. McNicol, J.H. De Bass, S.C. Kloet, J.W. Jenkins, J. Catal. 37 (1975) 424.
[53] F. Trifiro, A. Vaccari, O. Clause, Catal. Today 21 (1994) 185.
[54] J. Zielinski, Appl. Catal. A 94 (1993) 107.
[55] R. Lamber, G. Schulz-Ekloff, J. Catal. 146 (1994) 601.
[56] O. Clause, B. Rebours, E. Merlen, F. Triffiro, A. Vaccari, J. Catal. 73 (1991) 217.
[57] M. Jitianu, M. Bălăsoiu, R. Marchidan, M. Zaharescu, D. Crisan, M. Craiu, Int. J. Inorg. Mater. 2 (2000) 287.
[58] R. Villa, C. Cristiani, G. Groppi, L. Lieti, P. Forzatti, U. Cornaro, S. Rossini, J. Mol. Catal. A 204–205 (2003) 637.
[59] K. Schultze, W. Makowsky, R. Chyzy, R. Dziembaj, G. Geisman, Appl. Clay Sci. 18 (2001) 59.
[60] N.W. Hurst, S.J. Gentry, A. Jones, B.D. McNicol, Catal. Rev.-Sci. Eng. 24 (2) (1982) 233.
[61] E.R. Stobbe, B.A. de Boer, J.W. Geus, Catal. Today 47 (1999) 161.
[62] M. Ferrandon, J. Carnö, S. Järås, E. Björnbom, Appl. Catal. A 180 (1999) 141.
[63] F. Kapteijn, A. Dick van Langeveld, J.A. Moulijn, A. Andreïni, M.A. Vuurman, A.M. Turek, J.-M. Jehng, I.E. Wachs, J. Catal. 150 (1994) 94.
[64] F. Kapteijn, L. Singoredjo, A. Andreïni, J.A. Moulijn, Appl. Catal. B 3 (1994) 173.
[65] K.S. Chang, H. Song, Z.-S. Park, J.-W. Woo, Appl. Catal. A 273 (2004) 223.
[66] F. Kapteijn, G. Marban, J. Rodriguez-Mirasol, J.A. Moulijn, J. Catal. 167 (1997) 256.
[67] J. Nováková, M. Lhotka, Z. Tvarůžková, Z. Sobalík, Catal. Lett. 83 (2002) 215.
[68] V. Rives, M.A. Ulibarri, A. Montero, Appl. Clay Sci. 10 (1995) 83.
[69] F. Basolo, R.G. Pearson, Mechanisms of Inorganic Reactions, second ed., Wiley, New York, 1958, p. 146.
[70] S.L. Raj, B. Viswanathan, V. Srinivasan, J. Catal. 75 (1982) 185.
[71] A. Cimino, V. Indovina, F. Pepe, M. Schiavello, J. Catal. 14 (1969) 49.
[72] P. Beccat, J.C. Roussel, O. Clause, A. Vaccari, F. Trifirò, in: T.J. Dines, C.H. Rocheer, J. Thomson (Eds.), Catalysis and Surface Characterisation, The Royal Society of Chemistry, Cambridge, 1992, p. 32.
[73] P. Čuba, K. Kovanda, L. Hilaire, J. Balabánová, K. Jirátová, Appl. Catal., in press.